Chronic Pancreatitis or Pancreatic Tumor? A Problem-solving Approach

Kristy Marie Wolske, MD
Janardhana Ponnatapura, MD
Orpheus Kolokythas, MD
Lauren M. B. Burke, MD
Rafel Tappouni, MD
Neeraj Lalwani, MD

Certain inflammatory pancreatic abnormalities may mimic pancreatic ductal adenocarcinoma at imaging, which precludes accurate preoperative diagnosis and may lead to unnecessary surgery. Inflammatory conditions that may appear masslike include mass-forming chronic pancreatitis, focal autoimmune pancreatitis, and paraduodenal pancreatitis or "groove pancreatitis." In addition, obstructive chronic pancreatitis can mimic an obstructing ampullary mass or main duct intraductal papillary mucinous neoplasm. Secondary imaging features such as the duct-penetrating sign, biliary or main pancreatic duct skip strictures, a capsulelike rim, the pancreatic duct-to-parenchyma ratio, displaced calcifications in patients with chronic calcific pancreatitis, the "double duct" sign, and vessel encasement or displacement can help to suggest the possibility of an inflammatory mass or a neoplastic process. An awareness of the secondary signs that favor a diagnosis of malignant or inflammatory lesions in the pancreas can help the radiologist to perform the differential diagnosis and determine the degree of suspicion for malignancy. Repeat biopsy or surgical resection may be necessary to achieve an accurate diagnosis and prevent unnecessary surgery for inflammatory conditions.

Online supplemental material and DICOM image stacks are available for this article.

Abbreviations: AIP = autoimmune pancreatitis, CA = carbohydrate antigen, IPMN = intraductal papillary mucinous neoplasm, OCP = obstructive chronic pancreatitis, PDAC = pancreatic ductal adenocarcinoma, PDP = paraduodenal pancreatitis, SMA = superior mesenteric artery, SMV = superior mesenteric vein

RadioGraphics 2019; 39:1965–1982

https://doi.org/10.1148/rg.2019190011

Content Codes: CT GI MR OI

From the Departments of Radiology of Wake Forest Baptist Medical Center, 1 Medical Center Blvd, Winston-Salem, NC 27157 (K.M.W., J.P., R.T., N.L.); University of Washington, Seattle, Wash (O.K.); and University of North Carolina at Chapel Hill, Chapel Hill, NC (L.M.B.B.). Presented as an education exhibit at the 2018 RSNA Annual Meeting. Received February 4, 2019; revision requested March 25 and received April 22; accepted April 29. For this journal-based SA-CME activity, the author R.T. has provided disclosures; all other authors, the editor, and the reviewers have disclosed no relevant relationships. **Address correspondence to** N.L. (e-mail: *nlalwani@wakehealth.edu*).

SA-CME LEARNING OBJECTIVES

After completing this journal-based SA-CME activity, participants will be able to:

- Identify common inflammatory conditions that mimic PDAC.
- Describe imaging features that help in differentiating benign inflammatory masses from PDAC.
- Discuss the role of various imaging modalities in the visualization and differentiation of inflammatory pancreatic masses and pancreatic neoplasms.

See rsna.org/learning-center-rg.

Introduction

Pancreatic ductal adenocarcinoma (PDAC) is the fourth leading cause of death from cancer among men and women in the United States, with an overall mean 5-year survival rate of 8% and a mean survival rate for localized disease of 32% of patients (1). In 2018, more than 55 000 new cases of PDAC were diagnosed, and more than 44 000 people died of the disease (1). Although the Whipple procedure offers an improved survival rate for patients with localized resectable disease (mortality rate, <5%), morbidity from the Whipple procedure can be as high as 40%–50%, which makes preoperative identification of nonneoplastic pancreatic masses important (2,3). Equally important is avoiding delays in diagnosis that result in progression of undiagnosed PDACs that may rapidly become unresectable, leading to high mortality rates.

Three inflammatory entities commonly mimic PDAC at imaging: mass-forming chronic pancreatitis, focal autoimmune pancreatitis (AIP), and paraduodenal pancreatitis (PDP) or "groove pancreatitis" (4). In addition, obstructive chronic pancreatitis (OCP), with diffuse ductal dilatation and diffuse pancreatic parenchymal atrophy, can mimic ampullary masses or an intraductal papillary mucinous neoplasm (IPMN) of the main duct at imaging. In 5%–35% of Whipple

TEACHING POINTS

- Smooth narrowing of the pancreatic duct that traverses a pancreatic mass without abrupt obstruction strongly favors the diagnosis of an inflammatory mass.
- Pancreatic parenchymal calcifications are commonly seen in chronic pancreatitis, and peripheral displacement of calcifications can indicate a new underlying malignancy that may otherwise be imaging occult or poorly visualized because of gland heterogeneity from chronic pancreatitis.
- In the absence of the pathognomonic capsulelike rim, visualization of multiple pancreatic or biliary strictures rather than a solitary stricture and absence of substantial dilatation of the side branches or upstream pancreatic duct may be helpful clues that a focal mass in the pancreas represents focal AIP. Similar to other benign focal inflammatory lesions in the pancreas, AIP often shows the duct-penetrating sign, which further supports a benign diagnosis. Extrapancreatic autoimmune disease may be present.
- Displacement rather than encasement of the common bile duct and/or the gastroduodenal artery is highly suggestive of the diagnosis of PDP rather than PDAC.
- Dilatation of both the common bile duct and the main pancreatic duct, or the double duct sign, is highly suggestive of an underlying neoplasm. Although uncommon, inflammatory disease can produce this finding, which mimics malignancy.

procedures, the final pathologic diagnosis is a nonneoplastic inflammatory pancreatic mass (5). Although some patients with chronic inflammatory masses undergo the Whipple procedure for symptom management, others undergo pancreatic resection for high clinical suspicion for malignancy and concern that biopsies have yielded false-negative results.

Secondary imaging features such as the duct-penetrating sign, the presence of biliary or main pancreatic duct skip strictures, a capsulelike rim, the pancreatic duct-to-parenchyma ratio, displaced calcifications in patients with chronic calcific pancreatitis, the double duct sign, and vessel encasement or displacement may help to diagnose an inflammatory condition that may respond to medical management or PDAC, even when initial biopsy results showed a benign abnormality.

Clinical Background

Imaging findings, clinical presentation, risk factors, and laboratory findings overlap in patients with pancreatic inflammatory processes and those with a pancreatic neoplasm. A history of alcohol abuse and recurrent abdominal pain for at least 2 years is indicative of chronic pancreatitis; however, chronic pancreatitis is also a known risk factor for the development of PDAC, and the two entities can coexist in 1.8%–4% of patients (6–8). Serum tumor markers also overlap. A serum CA 19-9 level greater than 40 U/mL is 90% specific for a pancreatic malignancy (9–11). Unfortunately, serum CA 19-9 has only 81% sensitivity and therefore cannot exclude the diagnosis of malignancy. In addition, serum CA 19-9 may not be elevated until the disease is advanced (9).

The percutaneous false-negative biopsy rate for PDAC is as high as 60%, which further complicates the clinical management of pancreatic masses. (12,13). Endoscopic US-guided fine-needle aspiration has higher sensitivity but has a variable false-negative rate and has issues with nondiagnostic sampling (14). In a study by Fritscher-Ravens et al (15) in patients with normal pancreatic parenchyma and a focal mass, endoscopic US-guided fine-needle aspiration achieved sensitivity of 89%, specificity of 100%, and accuracy of 92%. However, in the same study, sensitivity for the detection of PDAC with endoscopic US-guided fine-needle aspiration was markedly lower when a mass was present in patients with chronic pancreatitis (sensitivity, 54%; specificity, 100%; and accuracy, 91%) (15). With these limitations, imaging continues to be important to the identification of alternative diagnoses and the guidance of clinical management when initial biopsy results are negative.

PDAC: A Brief Review

PDAC represents 94% of cancers arising from the exocrine pancreas (1) and is a hypovascular mass with extensive fibrosis at histopathologic examination (16), and these are also features of chronic focal inflammatory lesions. This histologic overlap may help to explain the difficulty in differentiating between the two entities.

At multiphase multidetector CT, classic PDAC is a hypoattenuating hypoenhancing mass with ill-defined margins. Multiple secondary signs of PDAC have been described and commonly include abrupt pancreatic duct cutoff, upstream pancreatic duct dilatation, upstream pancreatic parenchymal atrophy, and decreased enhancement in the distal pancreatic parenchyma (17). Ductal dilatation is seen in 80% of tumors in the head of the pancreas and in 50% of tumors in the body of the pancreas (16,18). In addition to ductal dilatation, the classic finding of upstream parenchymal atrophy is present in the majority of tumors (16). Decreased distal parenchymal enhancement was seen in almost 47% of patients in a study by Tamada et al (17).

At MRI, the classic appearance of PDAC is a hypointense mass at fat-suppressed T1-weighted MRI and variable signal intensity at T2-weighted MRI (19). At contrast-material–enhanced fat-suppressed T1-weighted MRI, PDAC typically shows hypoenhancement, which is particularly evident during the arterial phase (19,20). Diffusion restriction improves detection of small, ill-defined isointense masses from the normal pancreatic

parenchyma or adjacent obstructive pancreatitis (21,22). Diffusion-weighted MRI allows detection of pancreatic masses with similar sensitivity to that of gadolinium-enhanced MRI (23,24). PDAC often shows increased signal intensity at diffusion-weighted MRI (b >500 sec/mm^2) with relatively low apparent diffusion coefficients (25). However, diffusion restriction is not exclusive to PDAC and can be seen in conditions with inflammatory causes (eg, AIP) (26).

Isoattenuating masses that are not visualized discretely at routine multidetector CT are particularly difficult to diagnose, and they account for up to 10% of PDACs (27–29). Studies (30,31) have suggested that dual-energy CT may offer improved visualization of small PDACs. Specifically, low-voltage monoenergetic images that are reconstructed with noise reduction algorithms show improved tissue contrast compared with polychromatic images and may allow better visualization of small pancreatic tumors.

In the absence of a visualized mass at CT, focal pancreatic duct dilatation, mild peripancreatic infiltration, peritumoral cysts, or soft tissue around the celiac artery suggest the possibility of an occult malignancy (29,32). When a secondary sign is present without a visible mass, further investigation with MRI or endoscopic US should be recommended (16).

Additional findings including peritumoral cysts; persistent hypoenhancement during the arterial, portal venous, and delayed phases of contrast-enhanced MRI; and marked T1-weighted hypointensity similar to that of the renal medulla also were seen more commonly in PDAC than in focal chronic pancreatitis (22). In particular, peritumoral cysts, which appear as small irregular oval or linear areas of fluid signal intensity in the periphery of or adjacent to a mass, are highly suggestive of malignancy. In their study, Lee et al (22) saw peritumoral cysts in 84.5% of patients with PDAC and in 15.5% of those with focal chronic pancreatitis, with an odds ratio for association of peritumoral cysts with PDAC of 28.85. In comparison, abrupt pancreatic duct cutoff, which is widely considered a finding that is highly suspicious for PDAC, had an odds ratio of 9.07 in the same study. The cause of peritumoral cysts is uncertain, but they are thought to be secondary to obstruction of the side branches of the pancreatic duct from intraductal PDAC or adjacent desmoplasia.

In the evaluation of unexplained pancreatic duct strictures with upstream ductal dilatation, secondary signs also can be helpful. Findings of malignant stricture include duct enhancement at the transition site, abrupt transition without the duct-penetrating sign, segment strictures longer than 6 mm, and decreased attenuation in the upstream pancreatic parenchyma (32).

Mass-forming Chronic Pancreatitis

Background

In cases of chronic pancreatitis, 27%–50% of patients present with a localized mass or mass-forming pancreatitis, and 71% of focal lesions manifest in the pancreatic head (33,34). The typical patient history and risk factors including abdominal pain, weight loss, nausea, and jaundice commonly overlap with the patient history and risk factors of PDAC. CT may only allow accurate differentiation of mass-forming pancreatitis from PDAC in 77% of cases (35).

Imaging Features of Mass-forming Pancreatitis

At multidetector CT, both mass-forming pancreatitis and PDAC are typically hypoattenuating and hypoenhancing. The primary imaging features of mass-forming pancreatitis include an iso- or hypointense mass at T1-weighted MRI and an iso- or hyperintense mass at T2-weighted MRI, which are findings that are similar to those of PDAC. Fat-suppressed T1-weighted MRI sequences can provide increased lesion conspicuity compared with non–fat-saturation sequences, and mass-forming pancreatitis, similar to PDAC, typically is hypoenhancing at arterial phase contrast-enhanced MRI.

Imaging findings of chronic pancreatitis such as parenchymal calcifications and pseudocysts should raise the possibility that a focal mass represents focal inflammatory change (33,36,37). Additional findings favoring mass-forming pancreatitis over malignancy include the duct-penetrating sign, collateral branch duct dilatation, and a pancreatic duct-to-parenchyma ratio of less than 0.34 (4,38–40).

Duct-penetrating sign.—Smooth narrowing of the pancreatic duct that traverses a pancreatic mass without abrupt obstruction strongly favors the diagnosis of an inflammatory mass (39). The duct-penetrating sign is said to be present when the main pancreatic duct in the mass is seen in its entirety, without obstruction. The duct may be smoothly narrowed or of normal caliber. The duct-penetrating sign is 96% specific for an inflammatory pancreatic mass, with sensitivity of 85% and accuracy of 94% (39). Although the duct-penetrating sign can be seen at CT, it is better visualized at MR cholangiopancreatography (Fig 1).

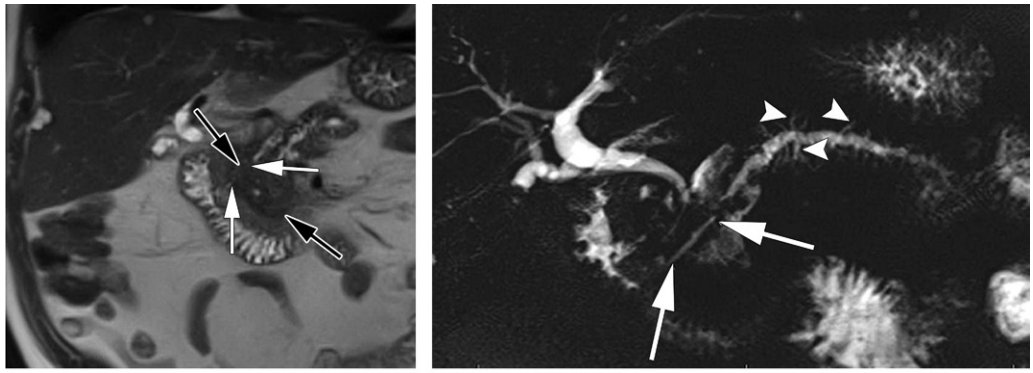

a. b.

Figure 1. Imaging findings that favor diagnosis of an inflammatory condition (or mass-forming pancreatitis) rather than malignancy. **(a)** Coronal T2-weighted MR image through the pancreatic head shows a heterogeneous masslike lesion (black arrows). The proximal main pancreatic duct has a decreased caliber and can be seen traversing through the mass (white arrows). **(b)** MR cholangiopancreatogram clearly shows the narrowed main pancreatic duct in the masslike lesion (arrows), which is consistent with the duct-penetrating sign. Prominent side branches are seen along the course of the distal pancreatic duct (arrowheads).

Collateral Duct Dilatation.—The presence of collateral duct or side-branch dilatation in the uninvolved or distal pancreas further supports an inflammatory cause (41,42). Dilatation of pancreatic duct side branches is thought to be secondary to a traction effect from fibrosis in a patient with chronic pancreatitis, rather than mass effect from a neoplasm, where duct obliteration would be expected (4).

Imaging Findings that Favor Malignancy

Certain imaging features such as a duct-to-parenchyma ratio greater than 0.34, displaced calcifications in a patient with chronic calcific pancreatitis, the double duct sign, vessel encasement, vessel deformity, and a superior mesenteric artery (SMA) to superior mesenteric vein (SMV) ratio of greater than 1 favor the diagnosis of PDAC (43–45).

Duct-to-Parenchyma Ratio.—The pancreatic duct-to-parenchyma ratio also can be helpful in determining the degree of suspicion for malignancy (41). At endoscopic US, a pancreatic duct-to-parenchyma ratio of greater than 0.34 strongly favors the diagnosis of PDAC (40). In patients with a pancreatic duct-to-parenchyma ratio of greater than 0.34, there is marked upstream pancreatic ductal dilatation with marked parenchymal atrophy, which are the imaging hallmarks of PDAC (Fig 2a). Relatively mild ductal dilatation with mild upstream parenchymal atrophy (pancreatic duct-to-parenchyma ratio, <0.34) raises the possibility of an inflammatory nonneoplastic cause (40).

Displaced Calcifications in Chronic Pancreatitis.—Pancreatic parenchymal calcifications are commonly seen in chronic pancreatitis, and peripheral displacement of calcifications can indicate a new underlying malignancy (Fig 2b) that may otherwise be imaging occult or poorly visualized because of gland heterogeneity from chronic pancreatitis (44,46).

The Double Duct Sign.—The junction of the pancreatic duct and the bile duct may be focally dilated in 70% of cases (ampulla of Vater) and eventually may be open in the major duodenal papilla (papilla of Vater). Therefore, an obstruction at the papilla or peripapillary region may give rise to dilatation of both ducts (47). Simultaneous dilatation of the common bile duct and pancreatic duct, known as the *double duct sign* (48,49), favors the diagnosis of a malignancy (Fig 2c).

Classically, the double duct sign is seen in PDACs involving the head of the pancreas and is seen in up to 77% of pancreatic head PDACs (37,50). However, the double duct sign is nonspecific and can develop secondary to inflammatory processes in the pancreas (eg, AIP) as well as other nonmalignant conditions (49).

Vessel Encasement and Vessel Deformity.—Soft-tissue attenuation that encases the adjacent vasculature is highly suggestive of the extraglandular spread of PDAC and is crucial in determining tumor resectability. In addition to vessel encasement, vessel caliber changes also are seen frequently, including circumferential vessel narrowing, occlusion, and vessel deformity. The *SMV teardrop sign*, a teardrop-shaped deformity of the SMV, is highly indicative of SMV encasement (43) (Fig 2d). Although uncommon, inflammatory conditions such as AIP may result in loss of fat planes with peripancreatic vessels or may have associated sclerosing mesenteritis or retroperito-

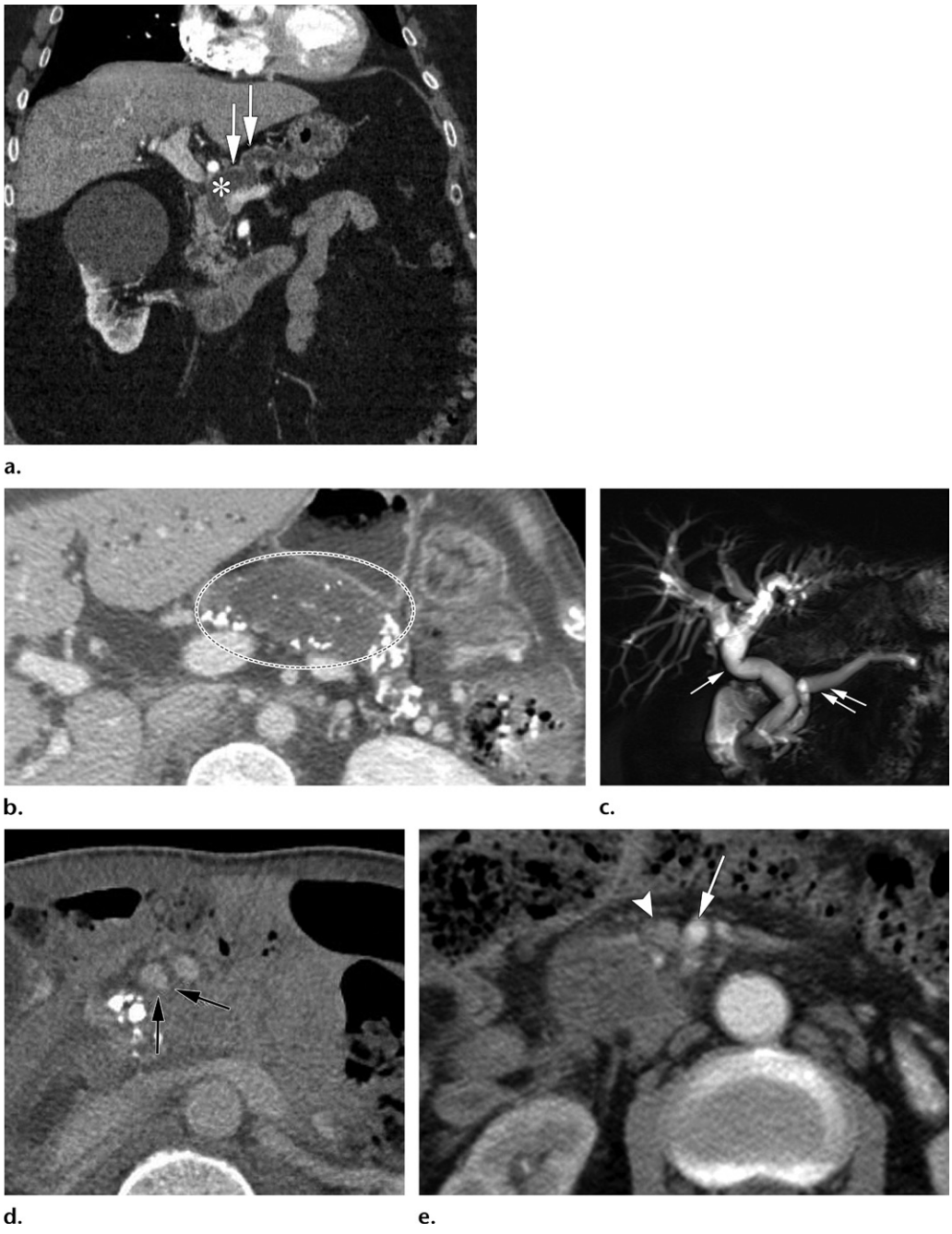

Figure 2. Imaging findings that favor diagnosis of a malignancy rather than an inflammatory condition. **(a)** Coronal CT image shows a duct-to-parenchyma ratio (maximum diameter of the diffusely dilated main pancreatic duct [∗] and the overlying atrophic parenchyma [arrows]) of greater than 0.5). **(b)** Axial CT image shows diffuse calcifications in the background parenchyma and peripheral displacement of calcifications by a focal hypoattenuating lesion (dotted circle) in the pancreatic body. **(c)** MR cholangiopancreatogram shows the double duct sign, or dilatation of both the pancreatic duct (double arrows) and the common bile duct (single arrow). **(d)** Axial CT image shows the teardrop sign (arrows), a teardrop-shaped deformity of the SMV due to vascular encasement. Note the loss of fat in the perivascular space. **(e)** Axial CT image shows the SMA-to-SMV ratio, or the decreased caliber of the SMV (arrowhead) (almost the same size as the SMA [arrow]), of greater than or equal to 1.0. Note the loss of fat in the perivascular space.

neal fibrosis mimicking extraglandular spread of pancreatic cancer (39,51).

SMA-to-SMV Ratio.—Enlargement of the SMA relative to the SMV with a ratio greater than or equal to 1.0 is an additional sign favoring the diagnosis of malignancy rather than an inflammatory process in the pancreas (44,45).

The release of vasoactive substances in pancreatitis is thought to increase regional blood flow, resulting in increased diameter of the distensible SMV compared with the adjacent SMA. Although

it is not well understood, the increase in the caliber of the SMA in patients with PDAC may be due to increased resistance to blood flow in the pancreas secondary to the presence of malignancy, or it may be due to wall thickening from perivascular invasion. The SMA-to-SMV ratio is not 100% sensitive or specific, but it can be considered a suspicious finding for PDAC if it is greater than 1 or if other signs also support the diagnosis.

Imaging Modalities for Mass-forming Pancreatitis

At transabdominal US, it is difficult to distinguish mass-forming chronic pancreatitis from PDAC because the imaging features overlap, and masses may be obscured by overlying bowel gas or the patient's body habitus (52,53). Endoscopic US offers improved visualization of masses and is used routinely to perform targeted biopsies. In masses with negative fine-needle aspiration results, contrast-enhanced endoscopic US may help to differentiate chronic pancreatitis from PDAC (54). A meta-analysis (55) of contrast-enhanced transabdominal and endoscopic US for evaluation of pancreatic masses found sensitivity of 89% and specificity of 84% for the diagnosis of PDAC when the lesion had a hypovascular hypoenhanced appearance. In the diagnosis of neoplastic lesions, sensitivity was 95% and specificity was 72% (55). Studies suggest that contrast-enhanced endoscopic US–guided fine-needle aspiration can help to identify hypoenhanced hypovascular areas for targeted biopsy and to avoid areas of probable necrosis (56). Similarly, US elastography has shown promise for diagnosis of pancreatic cancers, with sensitivity of 89.5% (57). Elastography combined with guided fine-needle aspiration may further improve results, with accuracy of 94.4%, sensitivity of 93.4%, and specificity of 100% (58). Overall, US elastography and contrast-enhanced endoscopic US can help to identify better sites for targeted fine-needle aspiration and to avoid false-negative results and necrotic areas.

Multidetector CT provides better visualization of pancreatic parenchymal calcifications than do US and MRI and allows better assessment of findings of calcification displacement due to a mass arising in a patient with chronic inflammation. Multidetector CT also provides excellent visualization of pancreatic parenchymal atrophy, duct structure, vessel encasement, and peripancreatic or metastatic spread of disease and allows assessment for staging and resection.

Compared with multidetector CT, MRI can be helpful for problem solving. MR cholangiopancreatography, especially with secretin, can be used to assess the main pancreatic duct for the duct-penetrating sign, the presence of which supports the diagnosis of an inflammatory mass (39,59,60). In cases of ductal dilatation without a visualized mass, MRI can provide better lesion detection than that of multidetector CT (61). The better soft-tissue contrast of MRI compared with that of multidetector CT can help in the identification and differentiation of small pancreatic tumors from other benign masslike lesions such as noninflammatory nonneoplastic pancreatic head hypertrophy and benign focal fatty infiltration of the pancreas (61). MR elastography can also help to differentiate malignancy from chronic inflammation. Liu et al (62) showed that a combination of 40-Hz MR elastography and dynamic contrast-enhanced MR imaging may help in the diagnosis of malignancy. They concluded that an enveloping neoplasm may exhibit higher stiffness than does chronic inflammation because of obvious fibrous tissue infiltration. However, these findings require more study.

PDAC versus Mass-forming Pancreatitis: A Practical Approach

None of the secondary signs of PDAC and mass-forming pancreatitis have 100% sensitivity or specificity. A diagnosis can be favored if more secondary imaging signs are present to support either a benign inflammatory process or a neoplastic process (Table 1; Table E1). Figures 3–6 show representative patients and provide a practical approach to diagnosis.

Autoimmune Pancreatitis

Background

Clinically, symptoms of AIP can mimic those of PDAC, with development of obstructive jaundice, acute or chronic abdominal pain, weight loss, and steatorrhea (63). AIP has classically been defined by elevated immunoglobulin 4 levels. Patients with PDAC occasionally show elevated immunoglobulin 4 levels, although they are uncommon. Elevated carcinoembryonic antigen and CA 19-9 levels are rarely seen in patients with AIP (64).

Two types of AIP have been described (Table 2): type 1 lymphoplasmacytic sclerosing pancreatitis and type 2 idiopathic duct-centric pancreatitis (65–69). Type 1 disease is characterized by elevated serum immunoglobulin 4 levels and is strongly (60%) associated with extrapancreatic autoimmune processes (65–67). The pancreatic involvement is typically diffuse (more than 60%), and approximately 85% of patients develop diabetes, which may be a clue to the diagnosis. Symptoms typically improve with administration of steroid therapy. Type 2 AIP can be more difficult to diagnose clinically, and the imaging findings can closely mimic PDAC (70). Type 2 AIP

Table 1: Summary of Imaging Findings of Mass-forming Pancreatitis and PDAC

Imaging Finding	Mass-forming Pancreatitis	PDAC	Comments
Duct-penetrating sign	May be present	Typically absent	Reliable sign of a benign abnormality (specificity, 96%; sensitivity, 85%), seen with mass-forming pancreatitis, AIP, and PDP
Collateral duct dilatation	May be present	Typically absent	Inflammation causes traction over the side branches and dilatation
Duct-to-parenchyma ratio >0.34	Typically absent	May be present	Smooth pancreatic ductal dilatation with an atrophic overlying parenchyma; reliable sign of malignancy (specificity, 97%; sensitivity, 94%)
Displaced calcifications	Typically absent	May be present	Mass evolving from preexisting chronic pancreatitis displaces the calcification toward the periphery
Double duct sign	Typically absent	May be present	Peripapillary obstruction (specificity, 63%–80%; sensitivity, 50%–76%)
SMA-to-SMV ratio >1	Typically absent	May be present	Peritumoral fatty infiltration may lead to deformity and decreased caliber of the SMV. Usually, the SMV is larger in diameter than the SMA. This sign, along with other supportive imaging signs, may help in making a diagnosis.
Vessel encasement or deformity	Typically absent	May be present	Occasionally, AIP can have perivascular inflammatory stranding mimicking PDAC

Note.—The online supplemental version of the table (Table E1) includes reference images.

may manifest with normal serum immunoglobulin 4 levels, and focal pancreatic involvement that closely mimics malignancy is seen in up to 85% of cases. Extrapancreatic solid organ autoimmune disease is also uncommon in type 2 AIP, with the exception of inflammatory bowel disease, which can be seen in 30% of cases and may be a clue to the diagnosis (Fig 7b).

In addition to extensive overlap of clinical and imaging features, a high false-positive biopsy rate for carcinoma further contributes to unnecessary surgical management in cases of AIP. At histologic evaluation, the rate of false-positive or suspected carcinoma is as high as 32% for biopsies and 41% for fine-needle specimens (71). Although AIP is uncommon, accounting for only 1.9%–6.6% of cases of chronic pancreatitis, it is the diagnosis in almost 25% of Whipple procedures performed for nonneoplastic causes (72).

Imaging Features of AIP

In the diffuse form of AIP, type 1, the classic imaging findings include diffuse sausage-like enlargement of the gland, a smooth contour, and loss of normal pancreatic lobulations. A low-attenuation halo or capsulelike rim is pathognomonic for AIP type 1 when present (Fig 7). Homogeneous contrast enhancement in both early and delayed phases is common (65,73). Reactive lymphadenopathy may be present, but calcifications and pseudocysts are typically absent. Areas of stenosis can develop in the pancreatic duct and the distal common bile duct because of inflammation.

In the absence of diffuse disease, the imaging appearance of focal AIP can closely mimic that of a neoplasm. The focal inflammatory mass may have indistinct margins, periglandular inflammation may mimic extrapancreatic spread of malignancy (39), and involvement of the common bile duct could result in a nonmalignant cause of the double duct sign (74,75). In the absence of the pathognomonic capsulelike rim, visualization of multiple pancreatic or biliary strictures rather than a solitary stricture and absence of substantial dilatation of the side branches or upstream pancreatic duct may be helpful clues that a focal mass in the pancreas represents focal AIP (76). Similar to other benign focal inflammatory lesions in the pancreas, AIP often shows the duct-penetrating sign, which further supports a benign diagnosis (77). Extrapancreatic autoimmune disease may be present (Fig 8).

Imaging Modalities for AIP

Multidetector CT readily shows the classic capsulelike rim seen in AIP, if it is present (Fig 7a). Invasion of malignancy in the extraglandular planes or vessel encasement are readily assessed with multidetector CT. Occasionally, inflammation of the periglandular fatty tissue may mimic extraglandular malignant soft-tissue invasion in patients with AIP, and this remains an imaging pitfall in the attempt to distinguish AIP from PDAC (39,51).

The classic halo or fibrotic rim seen in AIP is hypointense at T2-weighted MRI and shows

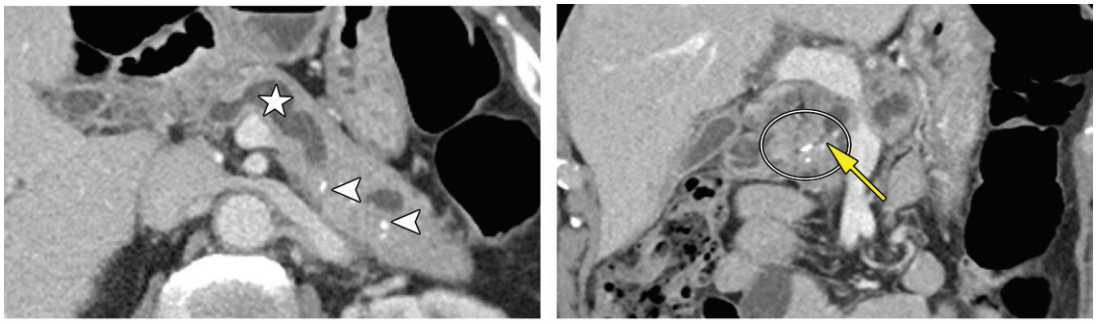

a. b.

Figure 3. Mass-forming chronic pancreatitis in the pancreatic head in a 49-year-old woman. **(a)** Axial CT image shows a dilated main pancreatic duct (☆). The overlying parenchyma is not atrophic and is well maintained. The duct-to-parenchyma ratio is less than 0.5. Scattered calcifications are seen in the parenchyma (arrowheads). **(b)** Coronal CT image shows a masslike lesion through the pancreatic head (circle). There is abrupt narrowing of the pancreatic duct, which penetrates through the parenchyma (arrow).

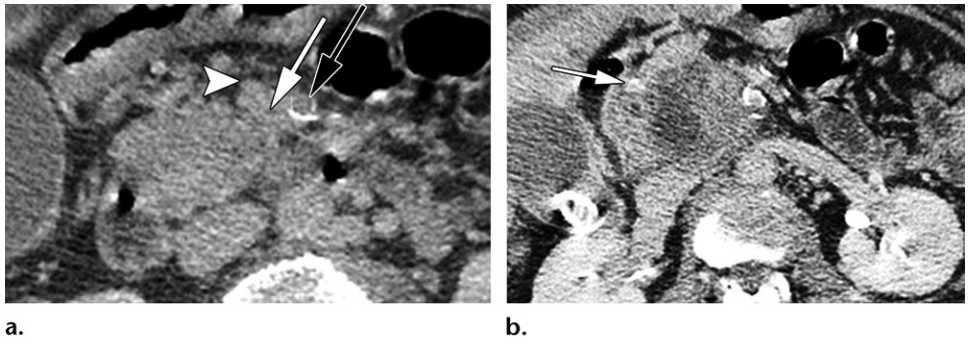

a. b.

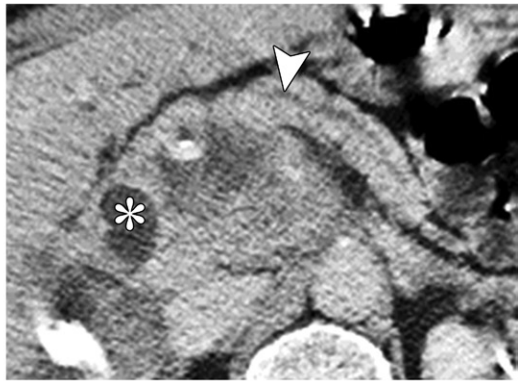

c.

Figure 4. PDAC of the pancreatic head in a 56-year-old man. **(a)** Axial CT image shows that the SMV (arrowhead) and SMA (black arrow) are of comparable size and that there is perivascular soft-tissue encasement (white arrow). The outline of the SMV is deformed. **(b)** Axial CT image shows a locally infiltrative hypoattenuating mass in the pancreatic head that is invading the gastroduodenal artery (arrow). **(c)** Axial CT image shows the normal caliber of the distal pancreatic duct and the well-maintained overlying parenchyma (arrowhead). Note the dilated distal common bile duct (*). No background parenchymal calcifications are shown.

weak enhancement at contrast-enhanced MRI (Fig 9a, 9b) (39). MR cholangiopancreatography shows either irregular stenosis in the main pancreatic duct or the duct-penetrating sign. Multiple pancreatic duct strictures or a concomitant common bile stricture is highly suggestive of AIP rather than malignancy and is best detected at MR cholangiopancreatography (77). Studies have shown improved visualization of the duct-penetrating sign and improved detection of multiple pancreatic duct strictures at secretin MR cholangiopancreatography (60). Incidental findings of inflammatory bowel disease (Fig 7b) or secondary sclerosing cholangitis with multiple biliary strictures may provide additional clues to the diagnosis of an underlying autoimmune inflammatory process (26,78).

Studies have also suggested a role for diffusion-weighted MRI in the detection and diagnosis of AIP and for monitoring response to therapy (59). For apparent diffusion coefficients of less than $1.26 \cdot 10^{-3}$ mm^2 per second, Hur et al (73) found sensitivity of 83% for the diagnosis of AIP and specificity of 79% for differentiating AIP from PDAC. Diffusion-weighted imaging alone does not allow AIP to be distinguished reliably from PDAC, and additional more specific imaging should be performed, when it is available.

Combining markedly decreased apparent diffusion coefficients with the presence of additional

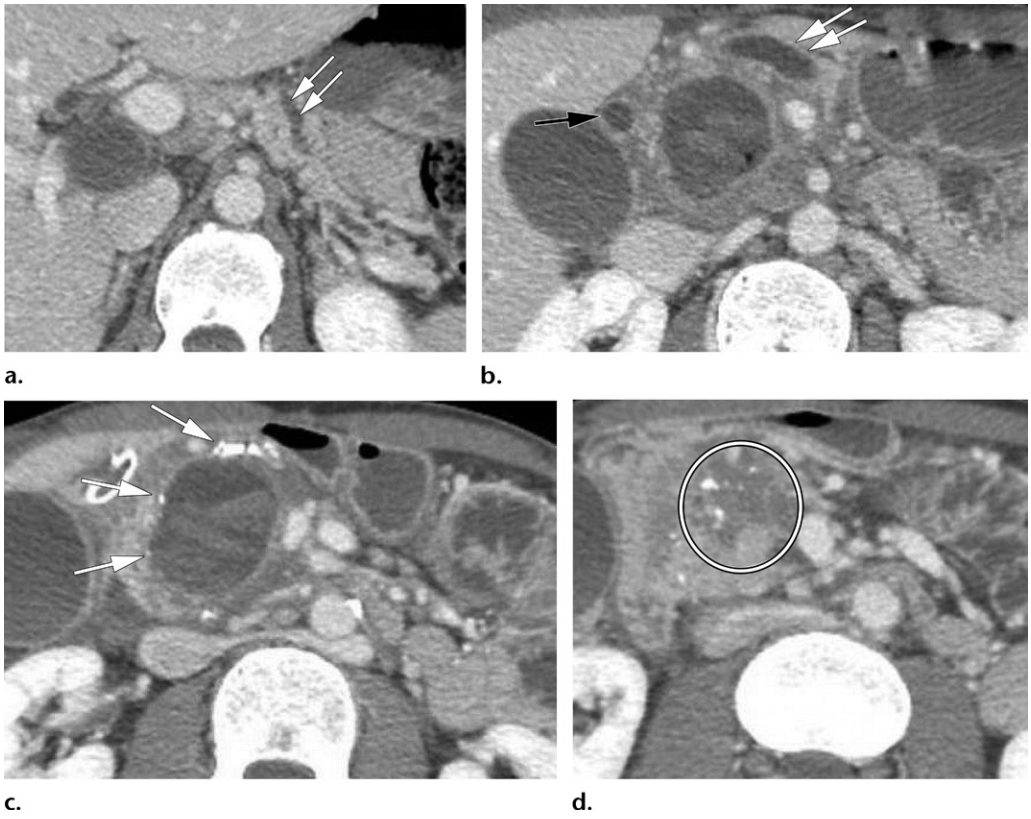

Figure 5. Mass-forming chronic pancreatitis with a pseudocyst in a 43-year-old man. **(a, b)** Axial CT images show a diffusely prominent main pancreatic duct (double arrows) and a dilated common bile duct (black arrow in **b**) representing the double duct sign. The overlying parenchyma is well maintained, and the duct-to-parenchyma ratio is less than 0.5. **(c)** Axial CT image shows scattered foci of calcifications in the pancreatic head (arrows). A cystic lesion in the pancreatic head shows hemorrhagic content, which is consistent with a pseudocyst. **(d)** Axial CT image shows the pancreatic head with a masslike enlargement (circle).

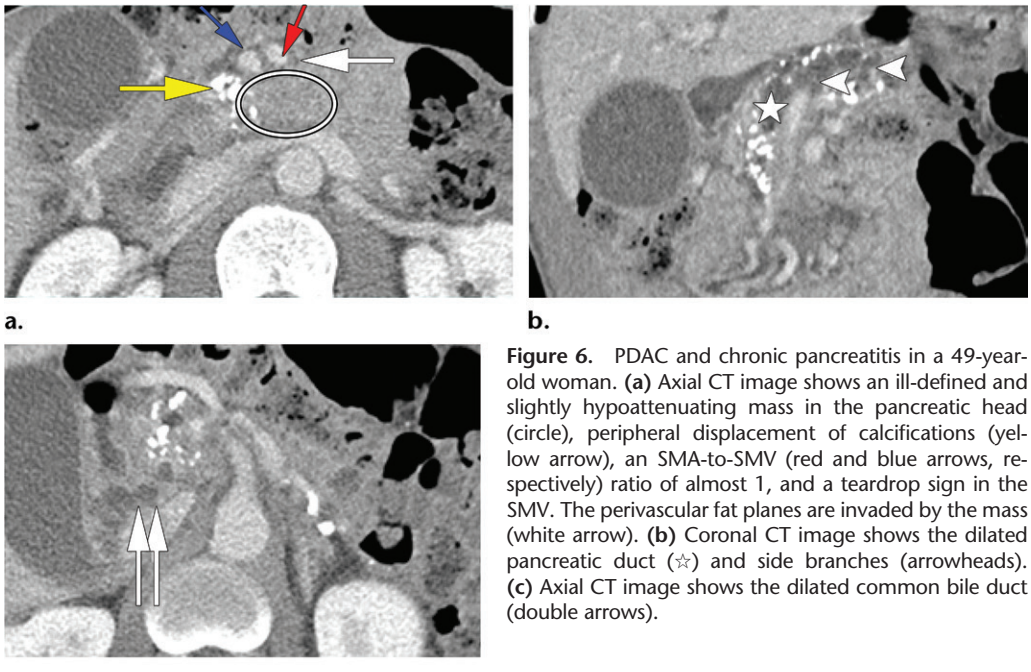

Figure 6. PDAC and chronic pancreatitis in a 49-year-old woman. **(a)** Axial CT image shows an ill-defined and slightly hypoattenuating mass in the pancreatic head (circle), peripheral displacement of calcifications (yellow arrow), an SMA-to-SMV (red and blue arrows, respectively) ratio of almost 1, and a teardrop sign in the SMV. The perivascular fat planes are invaded by the mass (white arrow). **(b)** Coronal CT image shows the dilated pancreatic duct (☆) and side branches (arrowheads). **(c)** Axial CT image shows the dilated common bile duct (double arrows).

Table 2: Types of AIP

Type 1: Lymphoplasmacytic sclerosing pancreatitis
Positive immunoglobulin 4 tissue staining results
Elevated serum immunoglobulin 4 level
Extrapancreatic organ involvement is common (60% of cases)
Inflammatory bowel disease in only 2%–6% of cases
Older patients (age usually >60 years), more common in men than in women
Pancreatic involvement is diffuse in 60% and focal in 40% of patients
Obstructive jaundice in 75% of cases
Patients may relapse after steroid therapy is completed
Type 2: Idiopathic duct-centric chronic pancreatitis
Immunoglobulin 4 tissue staining results are often negative
No elevation in serum immunoglobulin 4 level
No extrapancreatic solid organ involvement
Inflammatory bowel disease in 30% of cases
Younger patients (mean age, 43 years), equally common in men and women
Focal pancreatic lesion at imaging in 85% of cases
Obstructive jaundice in 50% of cases
Patients rarely relapse after steroid therapy is completed

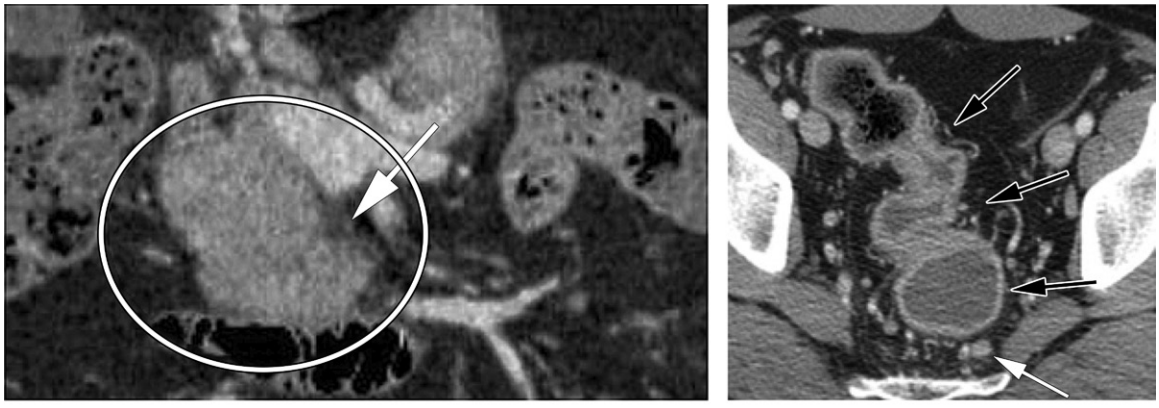

a. **b.**

Figure 7. Type 2 AIP in a 40-year-old man. **(a)** Contrast-enhanced coronal CT image through the pancreatic head shows a focal pancreatic head mass (circle). Note the smooth outline, the loss of normal pancreatic lobulations, and the hypoattenuating fibrotic rim (arrow). **(b)** CT image through the sigmoid colon shows mural thickening and associated hyperenhancement. Associated pericolonic hyperemia and vascular congestion (black arrows) and lymphadenopathy (white arrow) are also seen. Colonoscopy and biopsy findings were consistent with ulcerative colitis. (Full DICOM image stacks are available online for Fig 7a and 7b.)

signs can be helpful in diagnosis of AIP. For differentiating AIP from PDAC, studies have found that the capsulelike rim sign has specificity as high as 97%–100%; however, sensitivity is only 29% (73). Similarly, skip strictures in the common bile duct and the main pancreatic duct have been shown to have 100% specificity for AIP, but sensitivity is low, at 33% and 44%, respectively (73).

Perfusion-weighted MRI is also being investigated for the assessment of focal pancreatic lesions. The perfusion technique most widely used in abdominal imaging is dynamic contrast-enhanced MRI (59). Various quantitative parameters that may offer additional clues for differentiation of focal pancreatic lesions are currently under investigation. For example, early research shows a significant difference in time–signal-intensity curves, with PDAC typically showing type 2 time–signal-intensity curves with contrast enhancement followed by slow progressive enhancement, while focal chronic pancreatitis typically shows type 3 time–signal-intensity curves, with fast enhancement followed by a signal intensity plateau. Additional parameters including extravascular extracellular space volume fraction analysis were also found to be helpful for differentiation of chronic pancreatitis from PDAC, but further studies are needed to validate results from initial small trials (59,79,80). Figure 10 shows a diagnostic approach when AIP is suspected.

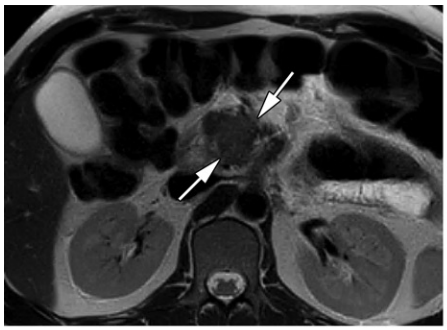

Figure 8. Type 2 AIP in a 42-year-old man. **(a)** Axial T2-weighted MR image through the proximal pancreas shows an ill-defined intermediate-signal-intensity masslike lesion (arrows). **(b)** Coronal T2-weighted MR image through the pancreatic head shows the narrowed caliber of the pancreatic duct traversing through the same region (arrow). Note coexisting focal stricture involving the distal common bile duct (arrowhead). **(c)** Axial contrast-enhanced delayed-phase MR image through the same region shows focal masslike lesion (arrowheads). The rest of the pancreas is unremarkable.

a.

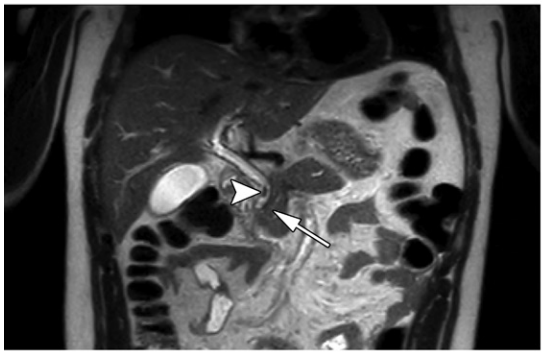

b.

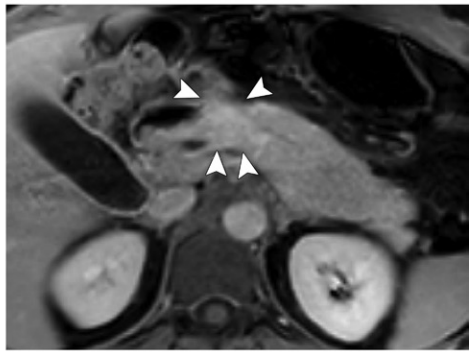

c.

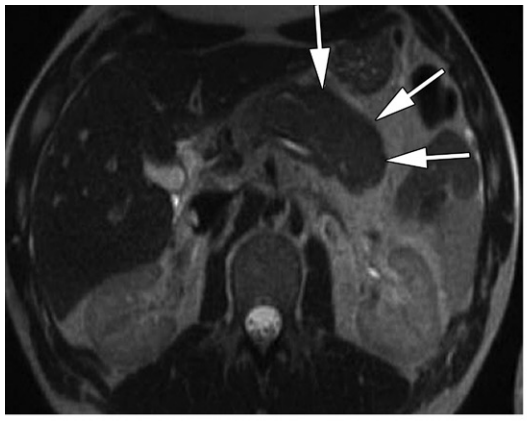

a.

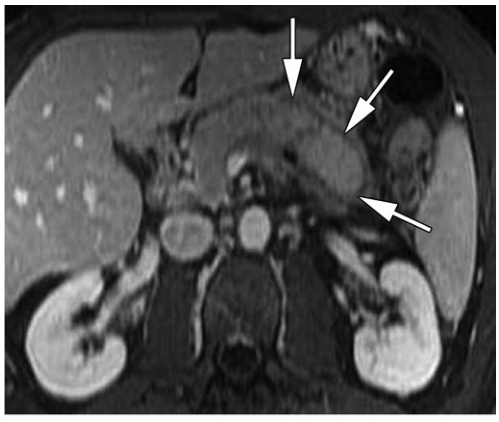

b.

Figure 9. Type 1 AIP in a 35-year-old woman. **(a)** Axial T2-weighted MR image shows a hypointense fibrotic rim (arrows). **(b)** Axial contrast-enhanced MR image shows a homogeneously enhancing pancreas and a nonenhancing fibrotic rim (arrows).

Management of AIP

The mainstay of therapy is administration of corticosteroids. Relapse is frequent in type 1 AIP but rare in type 2 AIP. Patients with steroid-refractory cases should be treated with immunomodulators in conjunction with steroids or rituximab (70).

Paraduodenal Pancreatitis

Background

PDP, also known as *groove pancreatitis* or *cystic duodenal dystrophy,* is a focal form of pancreatitis centered at the pancreaticoduodenal groove (81). The resulting inflammation or fibrosis can form a pseudotumor that may extend into the adjacent pancreatic head, mimicking locally invasive PDAC of the pancreatic head (82). Three distinct subtypes of PDP have been described (82), each with different imaging and histopathologic features. The solid tumoral type, or PDP type 1, manifests as a solid pseudotumor with minimal cystic change. Cysts may comprise less than 50% of the mass or may be completely absent. As described by Muraki et al (82), type 1 PDP may manifest as a solid-appearing sheetlike mass in the pancreaticoduodenal groove or a more rounded expansile lesion involving the pancreatic head. The expansile solid form, or subtype 1B, is particularly difficult to distinguish

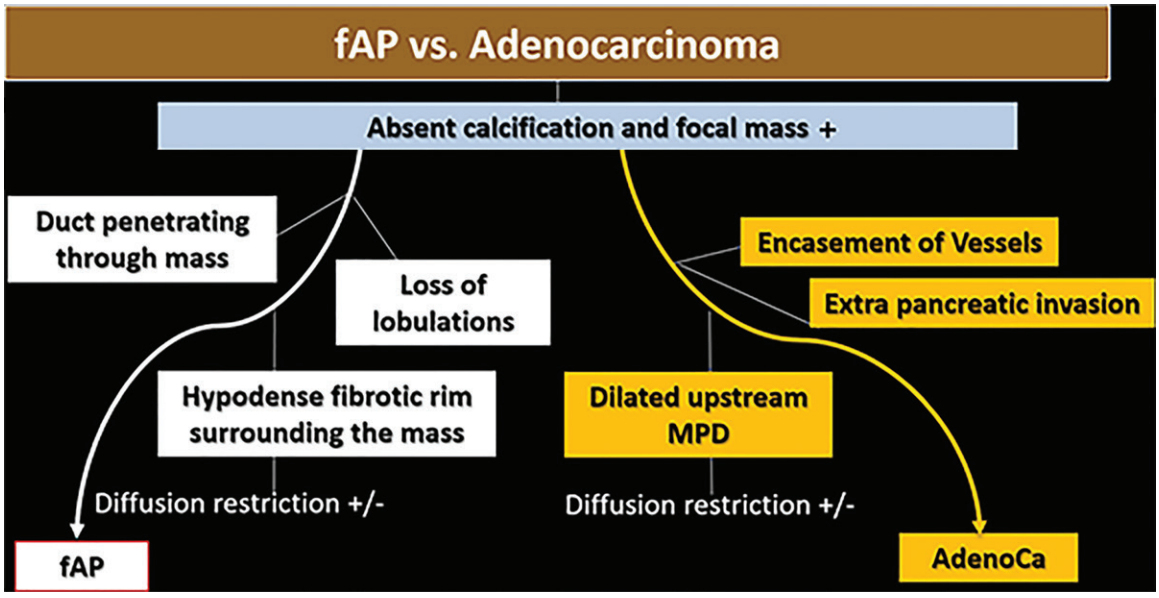

Figure 10. Diagnostic approach in a case of suspected AIP versus PDAC (+ signifies focal mass is present). *AdenoCa* = PDAC, *fAP* = focal AIP, *MPD* = main pancreatic duct.

from PDAC or a peripapillary neoplasm, given its round configuration, its solid appearance due to microcystic change or absent cysts, and the possibility of associated pancreatic parenchymal atrophy reported in 44% of patients with PDP type 1B in the study by Muraki et al (82). Much easier to identify because of the presence of cystic change in the pancreaticoduodenal groove is the cyst-forming subtype of PDP, or type 2 PDP, in which the lesions are predominantly cystic, with cysts accounting for greater than 80% of the lesion (82). The ill-defined type, or type 3 PDP, is not like a mass and is, therefore, less likely to mimic malignancy.

At resection of nonneoplastic pancreatic lesions, PDP was found in approximately 27% of cases, and as many as two-thirds of patients had a presurgical diagnosis of pancreatic or peripapillary cancer (82). Patients with PDP frequently experience severe chronic pain or duodenal outlet obstruction. Studies indicate that sustainable symptom relief can be achieved in more than two-thirds of patients who undergo medical or endoscopic treatment including sphincterotomy, pancreatic stent placement, or cyst drainage (82–86). Although studies have shown that the Whipple procedure allows successful management of pain and improves quality of life scores in most patients with PDP, given the morbidity associated with the procedure, accurate preoperative diagnosis preserves the opportunity for a trial of medical or endoscopic management (81,87).

Imaging Features of PDP

Key imaging features that suggest consideration of PDP in the differential diagnosis include a solid or solid and cystic mass centered at the pancreaticoduodenal groove, with involvement of the expected region of the accessory duct or accessory ampulla and medial duodenal wall thickening (81,82) (Fig 11). Cystic change should prompt consideration of PDP as the underlying diagnosis, with the understanding that up to 20% of patients have no visible cysts in the lesion (59). A sheetlike mass or *sandwich sign*, with a linear mass centered in the groove, is highly suggestive of type 1A PDP, even in the absence of visible cysts. A solid round tumoral subtype of PDP (type 1B "rice ball pattern" as described by Muraki et al [82]) exists and, in the absence of cystic change in the groove, is not reliably distinguishable from a peripapillary neoplasm or PDAC of the pancreatic head. The absence of biliary dilatation or a lack of substantial pancreatic parenchymal atrophy may suggest a nonneoplastic diagnosis (80). In addition, the presence of the duct-penetrating sign, thickening of the medial duodenal wall, or widening of the distance between the ampulla and duodenal lumen may suggest the diagnosis of PDP (88). Displacement rather than encasement of the common bile duct and/or the gastroduodenal artery is highly suggestive of the diagnosis of PDP rather than PDAC (4). In addition to the radiologic findings, clinical correlation may be helpful, because elevated CA 19-9 and overt jaundice are uncommon in PDP and are highly suggestive of PDAC.(88).

Imaging Modalities for PDP

At transabdominal US, PDP and PDAC may have similar appearances. However, at endoscopic US, identification of tiny cysts in the pancreaticoduodenal groove can suggest the diagnosis of PDP.

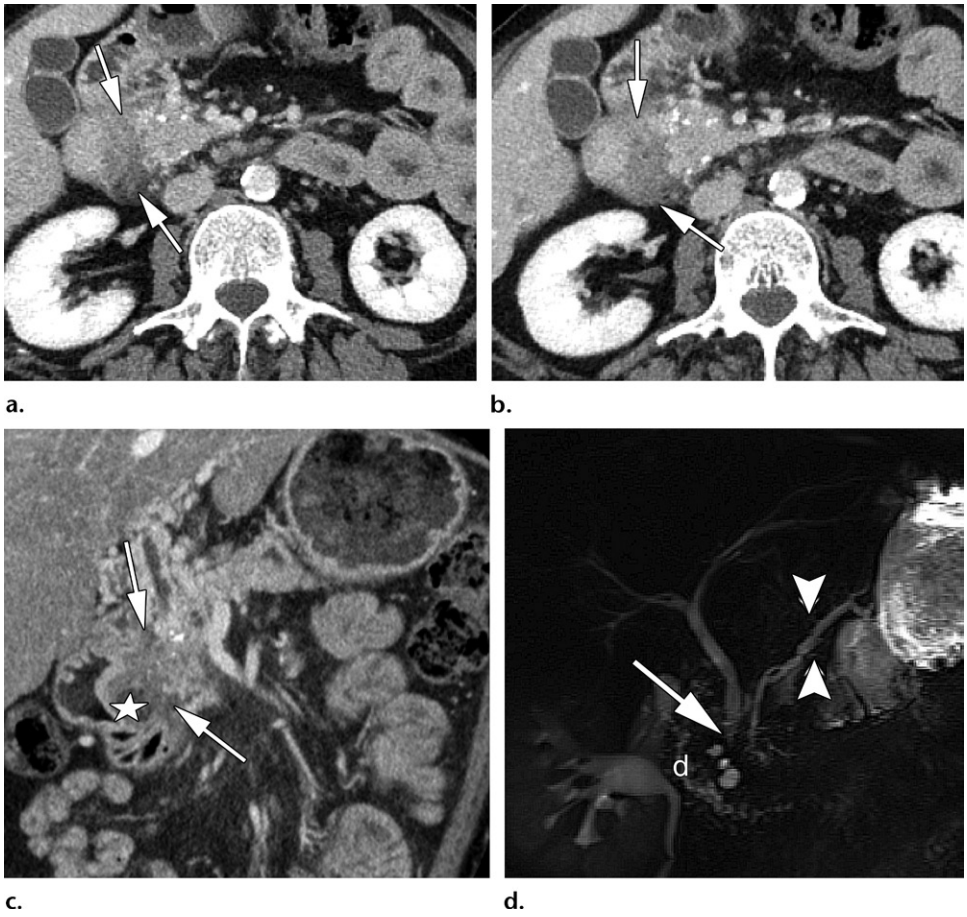

Figure 11. Type 1 solid PDP (groove pancreatitis) in a 39-year-old man. **(a, b)** Axial CT images show an ill-defined hypoattenuating masslike lesion in the duodenopancreatic groove (arrows). Scattered parenchymal calcifications appear in the pancreatic head. **(c)** Coronal CT image shows the extent of the masslike lesion in the duodenopancreatic groove (arrows) and associated cystic changes in the duodenal wall (☆). The distal common bile duct is partially visible. **(d)** MR cholangiopancreatogram shows focal narrowing of the distal common bile duct (arrow) and subtle prominence of the side branches (arrowheads). Note the widening of the duodenopancreatic groove and cystic changes in the duodenal wall *(d)*.

At multidetector CT, PDP mimics PDAC that involves the pancreaticoduodenal groove. PDP is hypointense during the arterial phase, with progressive late phase enhancement due to fibrosis, which is similar to PDAC. Visualization of a fat plane separating the mass from the pancreas may help exclude the pancreatic origin of the lesion. Multidetector CT can help in determining whether the adjacent distal common bile duct or adjacent vessels such as the gastroduodenal artery are encased, which supports the diagnosis of malignancy, or displaced, which supports the diagnosis of PDP (89,90).

Typically, the pancreaticoduodenal mass in patients with PDP is iso- or hypointense at T1-weighted MRI and iso- or hyperintense at T2-weighted MRI and can mimic PDAC. At T2-weighted MRI, microcysts in the mass that were not detected at multidetector CT suggest the diagnosis of PDP (Fig 12).

At MR cholangiopancreatography, PDP may cause smooth narrowing of the distal common bile duct and pancreatic duct, with widened distance between the ampulla and the duodenal lumen. Extensive fibrosis in the medial duodenal wall in PDP can lead to a nonmalignant cause of the double duct sign. In addition, MR cholangiopancreatography may allow visualization of subtle dilatation of the side branches or collateral duct, suggesting a chronic fibrotic or inflammatory process rather than malignancy. Secretin-enhanced MR cholangiopancreatography may improve visualization of the duct-penetrating sign in cases of PDP (91). Figure 13 shows an approach to use when diagnosis of PDP is suspected.

Obstructive Chronic Pancreatitis

Background

OCP is a subtype of chronic pancreatitis where the duct demonstrates a uniform contour and diffusely dilated appearance (92). At pathologic examination, OCP shows periductal fibrosis and subsequent ductal dilatation. Diffuse ductal changes may be secondary to chronic inflammatory stenosis of

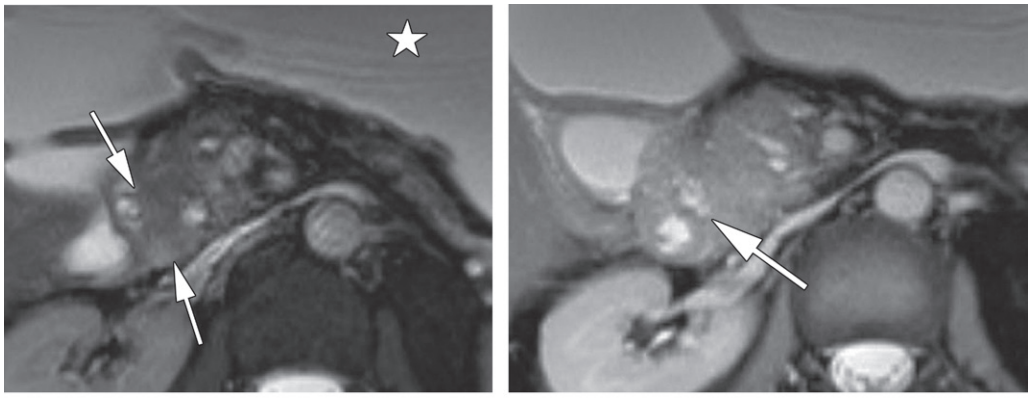

a. b.

Figure 12. Type 1 solid PDP (groove pancreatitis) in a 41-year-old man. **(a)** Axial fat-suppressed T2-weighted MR image shows an ill-defined masslike thickening of the medial duodenal wall, with intermediate signal intensity (arrows). At presentation, the patient was found to have duodenal outlet obstruction. Note the dilated stomach (☆). **(b)** Axial fat-suppressed T2-weighted MR image shows a predominantly solid masslike area in the pancreatic head and microcystic changes along the duodenal wall (arrow).

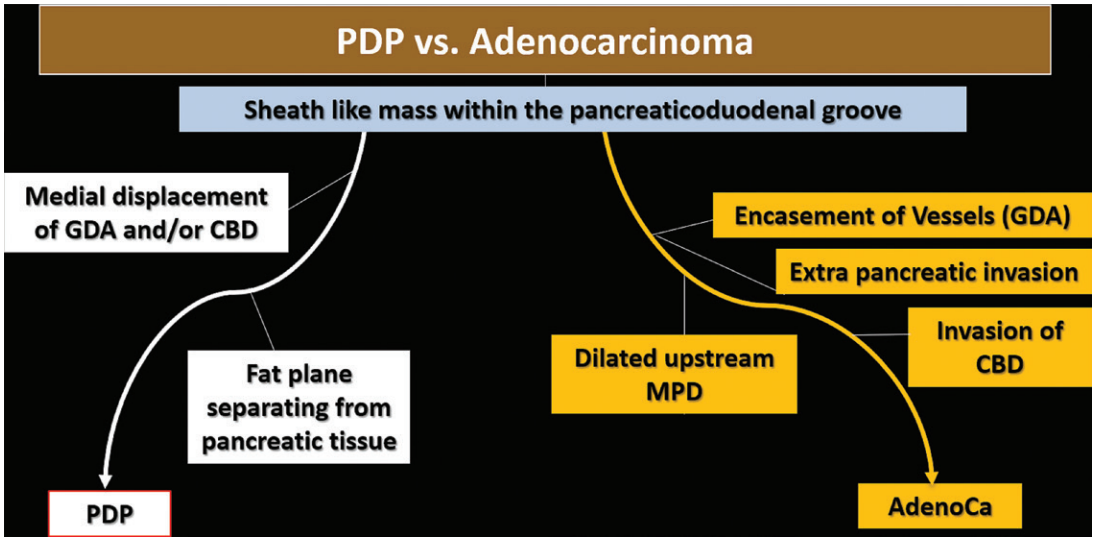

Figure 13. Diagnostic approach in a case of suspected solid variant PDP (groove pancreatitis) or PDAC. *AdenoCa* = adenocarcinoma, *CBD* = common bile duct, *GDA* = gastroduodenal artery, *MDP* = main pancreatic duct.

the papilla after repeated microtrauma due to the passage of stones and/or biliary sand, which leads to fibrosis and narrowing of the sphincter of Oddi and, eventually, the onset of OCP (46). Although protein inspissation may occur, pathologic changes in the ductal mucosa and calcification are infrequent. At gross examination, the pancreatic duct is dilated and there is variable parenchymal atrophy. At imaging, OCP may mimic juxtapapillary neoplasms (causing papillary obstruction) and main-duct IPMNs) (Table 3)(4).

OCP and Juxtapapillary Neoplasms

Slowly growing peripapillary tumors that cause obstruction and diffuse ductal dilatation may mimic OCP. These tumors include benign (eg, adenoma) and malignant (eg, PDAC and acinar carcinoma) neoplasms of the pancreas (93).

Imaging Modalities for OCP

Identifying small juxtapapillary neoplasms can prove difficult at imaging, especially at CT, even with contrast material administration, after which the tumor may appear isoattenuating when compared with the pancreatic parenchyma.

Few studies have shown that US and endoscopic US are more sensitive than CT in identifying small solid peripapillary or ductal lesions (94,95). Endoscopic US-guided fine-needle aspiration has been proposed as an option when a mass is detected at US or CT (96). Contrast-enhanced MRI seems to have the advantage over CT because of its better soft-tissue contrast definition (Fig 14a, 14b).

Dilatation of both the common bile duct and the main pancreatic duct, or the *double duct sign*, is highly suggestive of an underlying neoplasm. Although uncommon, inflammatory disease can pro-

Table 3: Differentiating among OCP, IPMN, and Juxtapapillary Neoplasms at Imaging

Imaging Features	OCP	IPMN	Juxtapapillary Neoplasms
Gland atrophy	Present or absent	Present/absent	Strongly present
Parenchymal calcification	Strongly present	Present/absent	Present or absent
Solid enhancing mass	Absent	Absent	Present
Double duct sign	Present or absent	Absent	Strongly present
Protrusion of major papilla into duodenum	Absent	Strongly present	Present or absent, with enhancing mass
Nodular enhancement along the wall of the pancreatic duct	Absent	Strongly present	Absent
Cystic ectasia of the branch ducts	Absent	Strongly present	Absent
Mucinous deposits within the ductal lumen	Absent	Strongly present	Absent

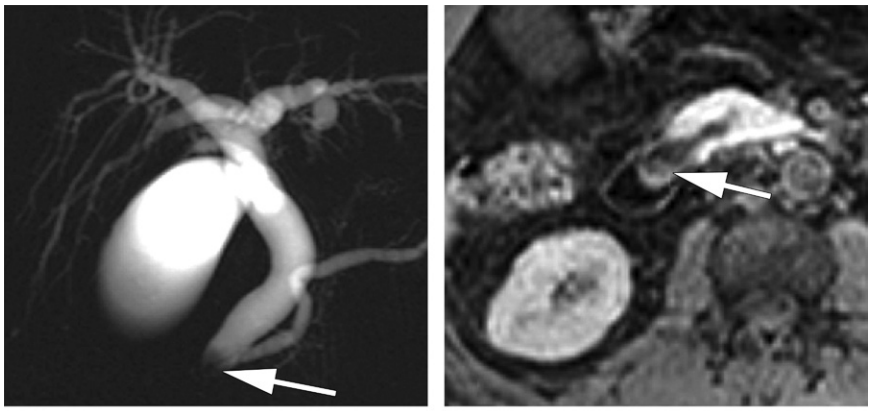

a. b.

Figure 14. Peripapillary neoplasm (adenoma) in a 42-year-old man. **(a)** MR cholangiopancreatogram shows a dilated biliary tree, a prominent pancreatic duct, and an ill-defined filling defect in the distal common bile duct (arrow). **(b)** Axial contrast-enhanced T1-weighted MR image shows a heterogeneous enhancing nodular lesion at the papilla (arrow).

duce this finding, which mimics malignancy (Fig 15a). Stones located in the main duct outlet at the papilla occasionally can be a nonmalignant cause of the double duct sign. In this case, MR cholangiopancreatography is the most sensitive and specific technique for diagnosis, and endoscopic retrograde cholangiopancreatography has a therapeutic role.

OCP and IPMN

Dilatation of the main pancreatic duct in the absence of an obstructing mass should suggest the diagnosis of main duct IPMN. Main duct IPMN has malignant potential and may require surgery, which makes it clinically important to distinguish IPMN from OCP (4,97).

Imaging of IPMN

At cross-sectional imaging, both OCP and IPMN may have atrophic changes in the pancreatic parenchyma in addition to main duct dilatation. Stones are frequently seen in OCP but are uncommon in IPMN (98). Mucinous deposits in the dilated main pancreatic duct that are seen in patients with IPMN are usually homogenous and have a similar appearance to that of ductal dilatation seen in patients with OCP: hypoechoic at US, hypoattenuating at multidetector CT, hyperintense at T2-weighted MRI, and hypointense at T1-weighted MRI (4). Thick mucinous deposits (if visualized) and papillary proliferations can appear similar at T2-weighted MRI (Fig 15a), as hypointense deposits along the duct wall. However, at contrast-enhanced imaging, unlike mucinous deposits, the papillary proliferations enhance and can help confirm the imaging diagnosis of IPMN (Fig 15b) (63). In addition to nodular enhancement along the duct wall, cystic ectasia of branch ducts also favors the diagnosis of IPMN. Although branch ducts may be dilated in OCP, they do not usually have a cystic structure.

Even in the absence of enhancing nodules along the duct wall, protrusion of the major papilla into the duodenum (the "fish-eye" appearance classically described at endoscopy) is pathognomonic for IPMN (Fig 15c). Ampullary PDAC also can cause papillary protrusion into the duodenum but can be differentiated from IPMN by the presence of an enhancing mass at the ampulla at cross-sectional imaging to avoid misdiagnosis.

Optical coherence tomography permits an evaluation of tissue microstructures by means of a high-resolution probe introduced into the main

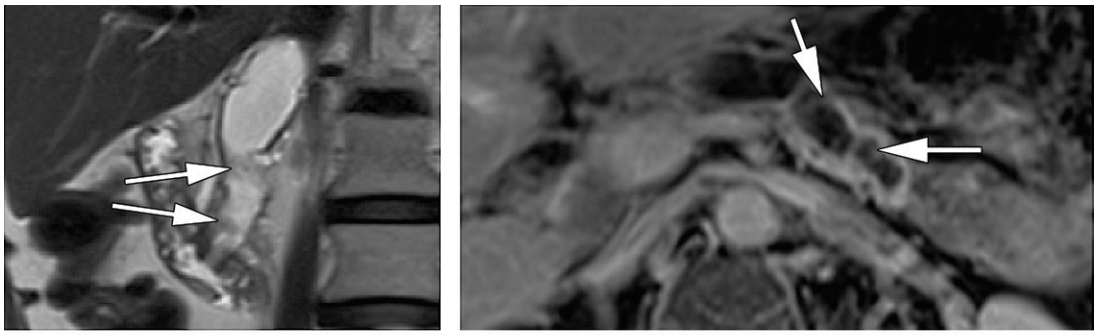

a. b.

c.

Figure 15. Main duct IPMN in a 53-year-old man. **(a)** Coronal T2-weighted MR image shows hypointense filling defects in the dilated main pancreatic duct (arrows). **(b)** Axial contrast-enhanced T1-weighted MR image shows nodular mural enhancement along the dilated main pancreatic duct (arrows). **(c)** Endoscopic image through the papillary region shows the classic protrusion of the major papilla into the duodenum (the "fish-eye" appearance).

pancreatic duct through an endoscopic retrograde cholangiopancreatographic catheter. Optical coherence tomography has shown high (almost 100%) accuracy for detection of malignant tissue compared with that of brush cytology (67.7%) (99).

Conclusion

Secondary imaging features may help to differentiate inflammatory from neoplastic masses in the pancreas. Imaging findings in correlation with serum CA 19-9 levels can help to guide clinical care and appropriate surgical treatment. However, no imaging feature or combination of features is 100% sensitive or specific for malignancy. The clinical and imaging features of neoplastic and nonneoplastic pancreatic masses overlap, and the entities can coexist in 1.8%–4% of cases. Chronic inflammation of the pancreas is a risk factor for developing PDAC, and background inflammatory changes can mask underlying malignancy and reduce the sensitivity and accuracy of endoscopic US-guided fine-needle aspiration. Further complicating image interpretation are cases of imaging-occult PDAC.

In conclusion, the imaging features of inflammatory masses and PDAC at CT and MRI have substantial overlap because both entities cause extensive fibrotic change. Therefore, secondary imaging findings such as the duct-penetrating sign, biliary or main pancreatic duct skip strictures, a capsulelike rim, the pancreatic duct-to-parenchyma ratio, displaced calcifications in chronic calcific pancreatitis, the double duct sign, and vessel encasement or displacement can provide valuable clues in the differential diagnosis of pancreatic masses and may help in avoiding unnecessary surgical morbidity and mortality for inflammatory conditions and delays in diagnosis of PDAC.

***Disclosures of Conflicts of Interest*.—R.T.** *Activities related to the present article:* disclosed no relevant relationships. *Activities not related to the present article:* consultancy for Behold AI. *Other activities:* disclosed no relevant relationships.

References

1. American Society of Clinical Oncology. Pancreatic Cancer: Statistics. https://www.cancer.net/cancer-types/pancreatic-cancer/statistics. Published 2018. Updated Janusary 2019. Accessed September 23, 2019.
2. Zakaria HM, Mohamed A, Alsebaey A, Omar H, Elazab D, Gaballa NK. Prognostic factors following pancreaticoduodenectomy for pancreatic ductal adenocarcinoma. Int Surg J 2018;5(12):3887–3882.
3. Klein F, Jacob D, Bahra M, et al. Prognostic factors for long-term survival in patients with ampullary carcinoma: the results of a 15-year observation period after pancreaticoduodenectomy. HPB Surg 2014;2014:970234.
4. Guarise A, Faccioli N, Morana G, Megibow AJ. Chronic Pancreatitis vs Pancreatic Tumors. In: Balthazar EJ, Megibow AJ, Pozzi Mucelli R, eds. Imaging of the Pancreas. Berlin, Germany: Springer, 2009; 329–369.
5. Kennedy T, Preczewski L, Stocker SJ, et al. Incidence of benign inflammatory disease in patients undergoing Whipple procedure for clinically suspected carcinoma: a single-institution experience. Am J Surg 2006;191(3):437–441.
6. Leung TK, Lee CM, Wang FC, Chen HC, Wang HJ. Difficulty with diagnosis of malignant pancreatic neoplasms coexisting with chronic pancreatitis. World J Gastroenterol 2005;11(32):5075–5078.
7. Tajima Y, Kuroki T, Tsutsumi R, Isomoto I, Uetani M, Kanematsu T. Pancreatic carcinoma coexisting with chronic pancreatitis versus tumor-forming pancreatitis: diagnostic utility of the time-signal intensity curve from dynamic contrast-enhanced MR imaging. World J Gastroenterol 2007;13(6):858–865.
8. Lalwani N, Mannelli L, Ganeshan DM, et al. Uncommon pancreatic tumors and pseudotumors. Abdom Imaging 2015;40(1):167–180.

9. Nazli O, Bozdag AD, Tansug T, Kir R, Kaymak E. The diagnostic importance of CEA and CA 19-9 for the early diagnosis of pancreatic carcinoma. Hepatogastroenterology 2000;47(36):1750–1752.
10. Ballehaninna UK, Chamberlain RS. Serum CA 19-9 as a Biomarker for Pancreatic Cancer-A Comprehensive Review. Indian J Surg Oncol 2011;2(2):88–100.
11. Xing H, Wang J, Wang Y, et al. Diagnostic Value of CA 19-9 and Carcinoembryonic Antigen for Pancreatic Cancer: A Meta-Analysis. Gastroenterol Res Pract 2018 Nov 21;2018:8704751.
12. Parsons L Jr, Palmer CH. How accurate is fine-needle biopsy in malignant neoplasia of the pancreas? Arch Surg 1989;124(6):681–683.
13. Rodriguez J, Kasberg C, Nipper M, Schoolar J, Riggs MW, Dyck WP. CT-guided needle biopsy of the pancreas: a retrospective analysis of diagnostic accuracy. Am J Gastroenterol 1992;87(11):1610–1613.
14. Lewitowicz P, Matykiewicz J, Heciak J, et al. Percutaneous fine needle biopsy in pancreatic tumors: a study of 42 cases. Gastroenterol Res Pract 2012;2012:908963.
15. Fritscher-Ravens A, Brand L, Knöfel WT, et al. Comparison of endoscopic ultrasound-guided fine needle aspiration for focal pancreatic lesions in patients with normal parenchyma and chronic pancreatitis. Am J Gastroenterol 2002;97(11):2768–2775.
16. Frampas E, Morla O, Regenet N, Eugène T, Dupas B, Meurette G. A solid pancreatic mass: tumour or inflammation? Diagn Interv Imaging 2013;94(7-8):741–755.
17. Tamada T, Ito K, Kanomata N, et al. Pancreatic adenocarcinomas without secondary signs on multiphasic multidetector CT: association with clinical and histopathologic features. Eur Radiol 2016;26(3):646–655.
18. Freeny PC, Marks WM, Ryan JA, Traverso LW. Pancreatic ductal adenocarcinoma: diagnosis and staging with dynamic CT. Radiology 1988;166(1 Pt 1):125–133.
19. Tamm EP, Bhosale PR, Vikram R, de Almeida Marcal LP, Balachandran A. Imaging of pancreatic ductal adenocarcinoma: State of the art. World J Radiol 2013;5(3):98–105.
20. Chandarana H, Babb J, Macari M. Signal characteristic and enhancement patterns of pancreatic adenocarcinoma: evaluation with dynamic gadolinium enhanced MRI. Clin Radiol 2007;62(9):876–883.
21. Park MJ, Kim YK, Choi SY, Rhim H, Lee WJ, Choi D. Preoperative detection of small pancreatic carcinoma: value of adding diffusion-weighted imaging to conventional MR imaging for improving confidence level. Radiology 2014;273(2):433–443.
22. Lee JH, Min JH, Kim YK, et al. Usefulness of non-contrast MR imaging in distinguishing pancreatic ductal adenocarcinoma from focal pancreatitis. Clin Imaging 2019;55:132–139.
23. Kartalis N, Lindholm TL, Aspelin P, Permert J, Albiin N. Diffusion-weighted magnetic resonance imaging of pancreas tumours. Eur Radiol 2009;19(8):1981–1990.
24. Ichikawa T, Erturk SM, Motosugi U, et al. High-b value diffusion-weighted MRI for detecting pancreatic adenocarcinoma: preliminary results. AJR Am J Roentgenol 2007;188(2):409–414.
25. Wang Y, Miller FH, Chen ZE, et al. Diffusion-weighted MR imaging of solid and cystic lesions of the pancreas. RadioGraphics 2011;31(3):E47–E64.
26. Sahani DV, Kalva SP, Farrell J, et al. Autoimmune pancreatitis: imaging features. Radiology 2004;233(2):345–352.
27. Ishigami K, Yoshimitsu K, Irie H, et al. Diagnostic value of the delayed phase image for iso-attenuating pancreatic carcinomas in the pancreatic parenchymal phase on multidetector computed tomography. Eur J Radiol 2009;69(1):139–146.
28. Prokesch RW, Chow LC, Beaulieu CF, Bammer R, Jeffrey RB Jr. Isoattenuating pancreatic adenocarcinoma at multi-detector row CT: secondary signs. Radiology 2002;224(3):764–768.
29. Kim JH, Park SH, Yu ES, et al. Visually isoattenuating pancreatic adenocarcinoma at dynamic-enhanced CT: frequency, clinical and pathologic characteristics, and diagnosis at imaging examinations. Radiology 2010;257(1):87–96.
30. Beer L, Toepker M, Ba-Ssalamah A, et al. Objective and subjective comparison of virtual monoenergetic vs. polychromatic images in patients with pancreatic ductal adenocarcinoma. Eur Radiol 2019;29(7):3617–3625.
31. Frellesen C, Fessler F, Hardie AD, et al. Dual-energy CT of the pancreas: improved carcinoma-to-pancreas contrast with a noise-optimized monoenergetic reconstruction algorithm. Eur J Radiol 2015;84(11):2052–2058.
32. Kim SW, Kim SH, Lee DH, et al. Isolated Main Pancreatic Duct Dilatation: CT Differentiation Between Benign and Malignant Causes. AJR Am J Roentgenol 2017;209(5):1046–1055.
33. Kim T, Murakami T, Takamura M, et al. Pancreatic mass due to chronic pancreatitis: correlation of CT and MR imaging features with pathologic findings. AJR Am J Roentgenol 2001;177(2):367–371.
34. Shinozaki M, Saisho H, Tokinaga K, et al. Tumor-forming pancreatitis on ultrasonography: follow-up study of the images and relation to clinical features [in Japanese] Jpn J Med Ultrason 1987;14(3):189–198. https://www.jsum.or.jp/journals/1364.
35. Liao Q, Zhao YP, Wu WW, Li BL, Li JY. Diagnosis and treatment of chronic pancreatitis. Hepatobiliary Pancreat Dis Int 2003;2(3):445–448.
36. Luetmer PH, Stephens DH, Ward EM. Chronic pancreatitis: reassessment with current CT. Radiology 1989;171(2):353–357.
37. Choueiri NE, Balci NC, Alkaade S, Burton FR. Advanced imaging of chronic pancreatitis. Curr Gastroenterol Rep 2010;12(2):114–120.
38. Karasawa E, Goldberg HI, Moss AA, Federle MP, London SS. CT pancreatogram in carcinoma of the pancreas and chronic pancreatitis. Radiology 1983;148(2):489–493.
39. Ichikawa T, Sou H, Araki T, et al. Duct-penetrating sign at MRCP: usefulness for differentiating inflammatory pancreatic mass from pancreatic carcinomas. Radiology 2001;221(1):107–116.
40. Eloubeidi MA, Luz LP, Tamhane A, Khan M, Buxbaum JL. Ratio of pancreatic duct caliber to width of pancreatic gland by endosonography is predictive of pancreatic cancer. Pancreas 2013;42(4):670–679.
41. Lin E, Alexander D. Focal Chronic Pancreatitis versus Pancreatic Cancer. In: Lin EC, Escott EJ, Garg KD, Bleicher AG, Alexander D, eds. Practical Differential Diagnosis for CT and MRI. New York, NY: Thieme, 2008; 212.
42. Busireddy KK, AlObaidy M, Ramalho M, et al. Pancreatitis-imaging approach. World J Gastrointest Pathophysiol 2014;5(3):252–270.
43. Hough TJ, Raptopoulos V, Siewert B, Matthews JB. Teardrop superior mesenteric vein: CT sign for unresectable carcinoma of the pancreas. AJR Am J Roentgenol 1999;173(6):1509–1512.
44. Elmas N. The role of diagnostic radiology in pancreatitis. Eur J Radiol 2001;38(2):120–132.
45. Elmas N, Oran I, Oyar O, Ozer H. A new criterion in differentiation of pancreatitis and pancreatic carcinoma: artery-to-vein ratio using the superior mesenteric vessels. Abdom Imaging 1996;21(4):331–333.
46. Graziani R, Tapparelli M, Malagò R, et al. The various imaging aspects of chronic pancreatitis. JOP 2005;6(1,Suppl):73–88.
47. Horiguchi S, Kamisawa T. Major duodenal papilla and its normal anatomy. Dig Surg 2010;27(2):90–93.
48. Ahualli J. The double duct sign. Radiology 2007;244(1):314–315.
49. Oterdoom LH, van Weyenberg SJ, de Boer NK. Double-duct sign: do not forget the gallstones. J Gastrointestin Liver Dis 2013;22(4):447–450.
50. Fulcher AS, Turner MAMR. MR pancreatography: a useful tool for evaluating pancreatic disorders. RadioGraphics 1999;19(1):5–24; discussion 41–44; quiz 148–149.
51. Ohara H, Nakazawa T, Sano H, et al. Systemic extrapancreatic lesions associated with autoimmune pancreatitis. Pancreas 2005;31(3):232–237.
52. Maringhini A, Ciambra M, Raimondo M, et al. Clinical presentation and ultrasonography in the diagnosis of pancreatic cancer. Pancreas 1993;8(2):146–150.
53. Karlson BM, Ekbom A, Lindgren PG, Källskog V, Rastad J. Abdominal US for diagnosis of pancreatic tumor: prospective cohort analysis. Radiology 1999;213(1):107–111.
54. Saftoiu A, Vilmann P, Bhutani MS. The role of contrast-enhanced endoscopic ultrasound in pancreatic adenocarcinoma. Endosc Ultrasound 2016;5(6):368–372.
55. D'Onofrio M, Biagioli E, Gerardi C, et al. Diagnostic performance of contrast-enhanced ultrasound (CEUS) and contrast-enhanced endoscopic ultrasound (ECEUS) for the

differentiation of pancreatic lesions: a systematic review and meta-analysis. Ultraschall Med 2014;35(6):515–521.
56. Seicean A, Badea R, Moldovan-Pop A, et al. Harmonic Contrast-Enhanced Endoscopic Ultrasonography for the Guidance of Fine-Needle Aspiration in Solid Pancreatic Masses. Ultraschall Med 2017;38(2):174–182.
57. Dyrla P, Gil J, Niemczyk S, Saracyn M, Kosik K, Czarkowski S, Lubas A. Elastography in the Diagnosis of Pancreatic Malignancies. Adv Exp Med Biol 2019;1133:41–48.
58. Facciorusso A, Martina M, Buccino RV, Nacchiero MC, Muscatiello N. Diagnostic accuracy of fine-needle aspiration of solid pancreatic lesions guided by endoscopic ultrasound elastography. Ann Gastroenterol 2018;31(4):513–518.
59. Siddiqui N, Vendrami CL, Chatterjee A, Miller FH. Advanced MR Imaging Techniques for Pancreas Imaging. Magn Reson Imaging Clin N Am 2018;26(3):323–344.
60. Manfredi R, Pozzi Mucelli R. Secretin-enhanced MR Imaging of the Pancreas. Radiology 2016;279(1):29–43.
61. Raman SP, Horton KM, Fishman EK. Multimodality imaging of pancreatic cancer-computed tomography, magnetic resonance imaging, and positron emission tomography. Cancer J 2012;18(6):511–522.
62. Liu Y, Wang M, Ji R, Cang L, Gao F, Shi Y. Differentiation of pancreatic ductal adenocarcinoma from inflammatory mass: added value of magnetic resonance elastography. Clin Radiol 2018;73(10):865–872.
63. Hammami M, Noomen F, Toumi O, et al. Autoimmune pancreatitis mimicking pancreatic cancer. N Am J Med Sci 2011;3(11):520–523.
64. Ghazale A, Chari ST, Smyrk TC, et al. Value of serum IgG4 in the diagnosis of autoimmune pancreatitis and in distinguishing it from pancreatic cancer. Am J Gastroenterol 2007;102(8):1646–1653.
65. Kamisawa T, Egawa N, Nakajima H, Tsuruta K, Okamoto A, Kamata N. Clinical difficulties in the differentiation of autoimmune pancreatitis and pancreatic carcinoma. Am J Gastroenterol 2003;98(12):2694–2699.
66. Okazaki K, Chiba T. Autoimmune related pancreatitis. Gut 2002;51(1):1–4.
67. Zamboni G, Lüttges J, Capelli P, et al. Histopathological features of diagnostic and clinical relevance in autoimmune pancreatitis: a study on 53 resection specimens and 9 biopsy specimens. Virchows Arch 2004;445(6):552–563.
68. Zhang L, Chari S, Smyrk TC, et al. Autoimmune pancreatitis (AIP) type 1 and type 2: an international consensus study on histopathologic diagnostic criteria. Pancreas 2011;40(8):1172–1179.
69. Madhani K, Farrell JJ. Management of Autoimmune Pancreatitis. Gastrointest Endosc Clin N Am 2018;28(4):493–519.
70. Lee LK, Sahani DV. Autoimmune pancreatitis in the context of IgG4-related disease: review of imaging findings. World J Gastroenterol 2014;20(41):15177–15189.
71. Learn PA, Grossman EB, Do RK, et al. Pitfalls in avoiding operation for autoimmune pancreatitis. Surgery 2011;150(5):968–974.
72. Abraham SC, Wilentz RE, Yeo CJ, et al. Pancreaticoduodenectomy (Whipple resections) in patients without malignancy: are they all 'chronic pancreatitis'? Am J Surg Pathol 2003;27(1):110–120.
73. Hur BY, Lee JM, Lee JE, et al. Magnetic resonance imaging findings of the mass-forming type of autoimmune pancreatitis: comparison with pancreatic adenocarcinoma. J Magn Reson Imaging 2012;36(1):188–197.
74. Bennett GL, Hann LE. Pancreatic ultrasonography. Surg Clin North Am 2001;81(2):259–281.
75. Menges M, Lerch MM, Zeitz M. The double duct sign in patients with malignant and benign pancreatic lesions. Gastrointest Endosc 2000;52(1):74–77.
76. Negrelli R, Manfredi R, Pedrinolla B, et al. Pancreatic duct abnormalities in focal autoimmune pancreatitis: MR/MRCP imaging findings. Eur Radiol 2015;25(2):359–367.
77. Boninsegna E, Manfredi R, Negrelli R, Avesani G, Mehrabi S, Pozzi Mucelli R. Pancreatic duct stenosis: Differential diagnosis between malignant and benign conditions at secretin-enhanced MRCP. Clin Imaging 2017;41:137–143.
78. Manfredi R, Frulloni L, Mantovani W, Bonatti M, Graziani R, Pozzi Mucelli R. Autoimmune pancreatitis: pancreatic and extrapancreatic MR imaging-MR cholangiopancreatography findings at diagnosis, after steroid therapy, and at recurrence. Radiology 2011;260(2):428–436.
79. Donati F, Boraschi P, Cervelli R, et al. 3 T MR perfusion of solid pancreatic lesions using dynamic contrast-enhanced DISCO sequence: Usefulness of qualitative and quantitative analyses in a pilot study. Magn Reson Imaging 2019;59:105–113.
80. Kim JH, Lee JM, Park JH, et al. Solid pancreatic lesions: characterization by using timing bolus dynamic contrast-enhanced MR imaging assessment--a preliminary study. Radiology 2013;266(1):185–196.
81. Kalb B, Martin DR, Sarmiento JM, et al. Paraduodenal pancreatitis: clinical performance of MR imaging in distinguishing from carcinoma. Radiology 2013;269(2):475–481.
82. Muraki T, Kim GE, Reid MD, et al. Paraduodenal Pancreatitis: Imaging and Pathologic Correlation of 47 Cases Elucidates Distinct Subtypes and the Factors Involved in its Etiopathogenesis. Am J Surg Pathol 2017;41(10):1347–1363.
83. Claudon M, Verain AL, Bigard MA, et al. Cyst formation in gastric heterotopic pancreas: report of two cases. Radiology 1988;169(3):659–660.
84. Mohl W, Hero-Gross R, Feifel G, et al. Groove pancreatitis: an important differential diagnosis to malignant stenosis of the duodenum. Dig Dis Sci 2001;46(5):1034–1038.
85. Procacci C, Graziani R, Zamboni G, et al. Cystic dystrophy of the duodenal wall: radiologic findings. Radiology 1997;205(3):741–747.
86. Arvanitakis M, Rigaux J, Toussaint E, et al. Endotherapy for paraduodenal pancreatitis: a large retrospective case series. Endoscopy 2014;46(7):580–587.
87. Casetti L, Bassi C, Salvia R, et al. "Paraduodenal" pancreatitis: results of surgery on 58 consecutives patients from a single institution. World J Surg 2009;33(12):2664–2669.
88. Mittal PK, Harri P, Nandwana S, et al. Paraduodenal pancreatitis: benign and malignant mimics at MRI. Abdom Radiol (NY) 2017;42(11):2652–2674.
89. Gabata T, Matsui O, Kadoya M, et al. Small pancreatic adenocarcinomas: efficacy of MR imaging with fat suppression and gadolinium enhancement. Radiology 1994;193(3):683–688.
90. Gabata T, Kadoya M, Terayama N, Sanada J, Kobayashi S, Matsui O. Groove pancreatic carcinomas: radiological and pathological findings. Eur Radiol 2003;13(7):1679–1684.
91. Chamokova B, Bastati N, Poetter-Lang S, et al. The clinical value of secretin-enhanced MRCP in the functional and morphological assessment of pancreatic diseases. Br J Radiol 2018;91(1084):20170677.
92. Witt H, Apte MV, Keim V, Wilson JS. Chronic pancreatitis: challenges and advances in pathogenesis, genetics, diagnosis, and therapy. Gastroenterology 2007;132(4):1557–1573.
93. Lévy P, Ruszniewski P. Chronic pancreatitis [in French]. Rev Prat 2002;52(9):997–1000.
94. Minniti S, Bruno C, Biasiutti C, et al. Sonography versus helical CT in identification and staging of pancreatic ductal adenocarcinoma. J Clin Ultrasound 2003;31(4):175–182.
95. Yasuda K, Mukai H, Nakajima M. Endoscopic ultrasonography diagnosis of pancreatic cancer. Gastrointest Endosc Clin N Am 1995;5(4):699–712.
96. Gerstenmaier JF, Malone DE. Mass lesions in chronic pancreatitis: benign or malignant? An "evidence-based practice" approach. Abdom Imaging 2011;36(5):569–577.
97. Tenner S, Carr-Locke DL, Banks PA, et al. Intraductal mucin-hypersecreting neoplasm "mucinous ductal ectasia": endoscopic recognition and management. Am J Gastroenterol 1996;91(12):2548–2554.
98. Ito K, Koike S, Matsunaga N. MR imaging of pancreatic diseases. Eur J Radiol 2001;38(2):78–93.
99. Perkins JD. Optical coherence tomography: expanding use in the bile duct. Liver Transpl 2007;13(5):765–768.